Biological Solitons in Biomembranes: Analytical Solutions of a Boussinesq-Type Equation with Amplitude-Dependent Nonlinearity

Fazal Abbas[1], Ali Raza[2,3,4], Fiazuddin Zaman[1,*] and Sajawal Abbas Baloch[3]

[1] Abdus Salam School of Mathematical Sciences, Government College University, Lahore, 54000, Pakistan

[2] Department of Mathematical Sciences, Stellenbosch University, Stellenbosch, 7600, South Africa

[3] National Institute for Theoretical and Computational Sciences (NITheCS), Stellenbosch, 7602, South Africa

[4] Centre for Mathematics and Statistical Sciences, Lahore School of Economics, Lahore, 54792, Pakistan

INFORMATION

Keywords:
Biomembranes
biological solitons
Jacobi elliptic function method
Khater method
Boussinesq-type equation
solitary waves

DOI: 10.23967/j.rimni.2025.10.75584

SCIPEDIA
Revista Internacional de Métodos Numéricos para Cálculo y Diseño en Ingeniería
RIMNI

Biological Solitons in Biomembranes: Analytical Solutions of a Boussinesq-Type Equation with Amplitude-Dependent Nonlinearity

Fazal Abbas[1], **Ali Raza**[2,3,4], **Fiazuddin Zaman**[1,*] and **Sajawal Abbas Baloch**[3]

[1]Abdus Salam School of Mathematical Sciences, Government College University, Lahore, 54000, Pakistan

[2]Department of Mathematical Sciences, Stellenbosch University, Stellenbosch, 7600, South Africa

[3]National Institute for Theoretical and Computational Sciences (NITheCS), Stellenbosch, 7602, South Africa

[4]Centre for Mathematics and Statistical Sciences, Lahore School of Economics, Lahore, 54792, Pakistan

ABSTRACT

Boussinesq-type equations (BTE) emerge in various fields of fluid and solid mechanics, particularly where nonlinearities and dispersion are considered. Boussinesq-type equations are used to model wave effects in biomembranes, particularly longitudinal waves. They can account for nonlinear and dispersive effects that are important for characteristic wave behavior in biomembranes, composed of lipids, with distinct nonlinear effects. This provides a realistic description of longitudinal mechanical waves in nerve membranes. In this research, we investigate the Boussinesq-type equation that describes the waves in biomembranes with amplitude-dependent nonlinearities, using the Khater method (KM) and the Jacobi elliptic function method (JEFM). In addition to producing generic biological answers, the proposed methods allow the analysis of single wave solutions. These methods make it easier to derive solutions for solitary waves, which occur in a variety of forms, including bell, anti-bell, periodic, anti-kink and kink solitons. Each of these waves has a wide range of possible applications in biomathematics. Some of the findings are displayed as contour, 2D, and 3D graphics with particular parameter values applied under the specified conditions in order to highlight the important propagation properties. To the best of our knowledge, the biological solitons of the considered model have not been reported by using the proposed techniques in the literature. These results provide new theoretical insights into wave phenomena in biomembranes and may contribute to biological physics and nonlinear science.

OPEN ACCESS

Received: 04/11/2025

Accepted: 15/12/2025

Published: 23/01/2026

DOI
10.23967/j.rimni.2025.10.75584

Keywords:
Biomembranes
biological solitons
Jacobi elliptic function method
Khater method
Boussinesq-type equation
solitary waves

1 Introduction

Nonlinear evolution equations (NLEEs) play a vital role in numerous real-world scenarios, capturing the complexities of dynamic systems. These equations are fundamental for understanding fluid dynamics, as they clarify wave generation and turbulence. In the field of optics, the behavior of light in nonlinear media is represented, leading to phenomena such as solitons—stable, solitary wave packets. Additionally, nonlinear evolution equations are present in biology, shedding light on population

*Correspondence: Fiazuddin Zaman (f.zaman@sms.edu.pk).

dynamics and the spread of diseases. In finance, they aid in modeling market dynamics and valuing options. Their applications span various fields of mathematics and physics [1–3]. These equations are crucial for understanding systems where linear approximations fail. They provide significant insights into the intricate patterns and structures that arise in both nature and technology. Solitons in NLEEs hold significant importance due to their distinctive characteristics and wide-ranging applications across various scientific disciplines. These stable and concentrated wave packets emerge from the intricate relationship between nonlinearity and dispersion in NLEEs. Unlike traditional waves, solitons maintain their shape and velocity over long distances and remain unaffected by interactions with other solitons. This inherent stability makes them essential for modeling and comprehending complex physical phenomena. Their robustness and stability during interactions make solitons valuable tools for tackling and investigating NLEEs, providing valuable insights into the dynamics of complex, real-world systems. A range of methods is utilized to explore accurate soliton solutions in various domains, such as the the Lie symmetry approach [4,5], unified approach [6,7], Hirota bilinear [8,9], modified Sardar sub equation [10], generalized Riccati equation mapping [11,12], and many more [13,14].

Recent studies have explored modeling and simulation in applied sciences. Wang et al. [15] examined friction in nanofibrous membranes, Yu et al. [16] simulated fluid structure interactions, and Liu et al. [17] developed a noise tolerant neural network for chaotic system synchronization. These studies highlight the importance of solving complex NLPDEs in engineering and nonlinear dynamical systems. Tang et al. [18], Su et al. [19], and Hassan et al. [20] reviewed biological systems and immune responses, where dynamical models can describe processes such as bacterial detection, and modulation of immune response. In physics and engineering, Zhang et al. [21] explored nonlinear vectorial optics in nematic fluids, while Qiao et al. [22] analyzed celestial dynamics of the Earth–Moon system using Hamiltonian methods. Additionally, Guo et al. [23] proposed high-performance computational designs that benefit from accurate modeling of dynamic systems. These studies highlight the importance of analytical and numerical methods for understanding complex dynamical phenomena.

The renowned wave equation, which is founded on the principle of momentum conservation, describes motion at a finite speed. To incorporate related physical phenomena, modifications to the wave equation are necessary. In conservative systems, BTE are commonly employed. The initial Boussinesq equation was formulated for surface waves on a fluid layer [24]; however, these equations are now also applicable in solid mechanics [25]. The primary characteristics of Boussinesq-type equations include: (i) bi-directionality; (ii) nonlinearity of any order; (iii) dispersion of any order. In addition to fluid mechanics, numerous studies have been conducted on such equations that are derived from various physical assumptions [26–30]. In the field of solid mechanics, nonlinearity arises from the nonlinear relationship between stress and strain, as well as the nonlinear strain tensor, indicating the involvement of both physical and geometrical nonlinearities [31]. Consequently, the governing equations incorporate terms of the $\frac{\partial v_i}{\partial x_j}$ type (where i and $j = 1, 2, 3$), meaning that the gradients of displacement are included in the model. For instance, the simple 1D equation is given by

$$v_{tt} - d_0^2 (1 + kv_x) v_{xx} = 0, \tag{1}$$

where k is the nonlinear parameter and d_0 is the velocity in unperturbed state. The velocity d_0 is calculated as

$$d^2 = d_0^2 (1 + kv_x) . \tag{2}$$

In solids, the dispersive effects are caused by either the microstructure [32] or the geometry. Then in the proposed equation, the terms v_{xxxx} and v_{xxtt} occur. The interaction of nonlinear and dispersive effects can lead to the formation of solitary waves. Over the past ten years, there has been a rapid increase in interest regarding mechanical waves in biomembranes [33]. Biomembranes possess a unique structure composed of lipids, and in this context, the nonlinear effects differ from those observed in solid materials. According to experimental findings, the nonlinearity present in biomembranes can be described in terms of velocity.

$$d^2 = d_0^2 + pv + qv^2, \tag{3}$$

where v is the density change along the biomembrane's axis and p and q are coefficients. Heimburg-Jackson model, which accounts for these nonlinearities in addition to the dispersive term or terms. Solitary waves may then form as a result of the governing equation, which is of the Boussinesq type. In this study, the improved Heimburg-Jackson model is studied by using Khater method and JEFM. These techniques make it possible to convert partial differential equations into ordinary differential equations, which makes it easier to construct analytical solutions. These techniques allow for the derivation of various soliton and periodic solutions and are easy to apply to higher-order NLPDEs. Nevertheless, a drawback of these methods lies in the possible complexity encountered when applying them to higher-dimensional systems or more complex nonlinear models. Nevertheless, the findings provide a useful framework for more research on NLPDEs in a variety of contexts. To the best of our knowledge, this is the first work to obtain the soliton solutions of the improved Heimburg–Jackson Boussinesq-type equation using both the Khater method and the JEFM. Boussinesq-type equations describe how waves propagate through lipid bilayers. These equations address both the wave's compressibility as a result of lipid bilayer properties and the wave's dispersive nature through the lipid bilayer's micro-structural properties. However, only limited analytical solutions have been produced for the proposed model. As a result, our understanding of the physical behavior of nonlinear waves in biomembranes is not yet completely understood. As such, this paper presents the results of a study that is conducted for deriving exact soliton using two analytical techniques. The remaining work is adjusted as follows: In Section 2, the derivation of proposed model is given. In Section 3, we will discuss the description of the proposed techniques. While the extraction of solutions is explained in Section 4, the obtained solutions are graphically shown in Section 5. Finally, Section 6 provides the concluding remarks.

2 Derivation of the Proposed Model

The propagation of signals within a nerve fiber is a complex process. The nerve fiber can be represented as a tube filled with axoplasm and surrounded by extracellular fluid. The tube's wall consists of a biomembrane [34]. This biomembrane is a unique biological structure composed of phospholipids with their hydrophobic tails oriented inward, away from both intracellular and extracellular fluids [35]. In general terms, the lipid membrane serves as a specialized biological microstructure with intricate properties. In general, the lipid membrane serves as a unique biological microstructure characterized by complex properties. The ion concentration inside and outside a fiber varies; however, ion exchange can take place through ion channels. These channels remain closed at rest but can be activated by electrical or mechanical stimuli. The electrophysiological model that describes the propagation of an electrical signal known as the action potential was developed by Hodgkin and Huxley in [36]. This model is founded on telegraph equations and the dynamics of ion channels opening and closing in response to electrical stimuli. Nevertheless, it fails to account for all the intricate effects observed in nerve fibers. Research conducted by Iwasa et al. in [37] and Tasaki in [38] has convincingly shown the swelling of the adjacent biomembrane along with the associated heat exchange. This indicates that the action potential is also accompanied by a mechanical wave within the fiber wall. A mathematical framework that governs such a wave has been proposed by Heimburg and

Jackson. Their model is founded on the wave equation, specifically on the equilibrium of momentum, and is expressed in relation to the change in density $\Delta\rho_A = v$ along the longitudinal axis:

$$v_{tt} = \left(d^2 u_x\right)_x. \tag{4}$$

Two fundamental assumptions are established. Firstly, it is presumed that the velocity d of a wave within a circular biomembrane is associated with the compressibility of the lipid structure and can be regarded as

$$d^2 = d_0^2 + pv + qv^2, \tag{5}$$

where p and q are coefficients and d_0 is the velocity sound wave. The second assumption involves incorporating the higher order term into the governing equation kv_{xxxx}, which is responsible for dispersion. Consequently, the governing equation is then

$$v_{tt} = \left[\left(d_0^2 + pv + qv^2\right) v_x\right]_x - k_1 v_{xxxx}, \tag{6}$$

where k is constant. Eq. (6) represents a Boussinesq-type equation. Heimburg and Jackson have shown that Eq. (6) has a solitary pulse-type solution. Numerous additional studies have examined such solutions [39–41]. The Eq. (6) is modified to address the issue of unbounded velocities at higher frequencies. In accordance with the concepts derived from solid mechanics and reinforced by the Lagrangian formalism, the inertial term is incorporated into the governing equation:

$$v_{tt} = \left[\left(d_0^2 + pv + qv^2\right) v_x\right]_x - k_1 v_{xxxx} - k_2 v_{xxtt}, \tag{7}$$

where $k_1 v_{xxxx}$ represents elastic dispersion associated with the curvature and bending resistance of the lipid bilayer and $k_2 v_{xxtt}$ reflects inertial dispersion due to the microstructure of the membrane and prevents nonphysical high-frequency instabilities. From the perspective of solid mechanics, the significance of the fourth order mixed derivative is not unexpected, as it is widely recognized that the inclusion of solely spatial derivatives in the governing equation can result in instabilities. Furthermore, the mixed fourth order derivative is associated with the inertia of the microstructure. Maurin and Spadoni [42] have demonstrated that both dispersive terms emerge naturally when all factors related to wave propagation in solids are taken into account, a finding that has also been validated through experimental means [43].

The nerve fiber can be modeled as a cylindrical structure with axoplasm inside and a lipid bilayer membrane on the surface, as shown in Fig. 1. This biological configuration motivates the nonlinear dispersive model described in this work.

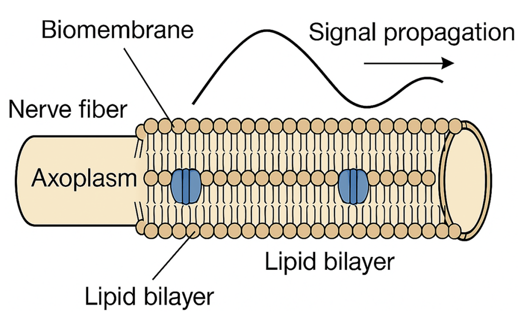

Figure 1: Schematic representation of a nerve fiber surrounded by a biomembrane, highlighting the lipid bilayer and signal propagation direction

3 Description of Analytical Techniques

3.1 Khater Method

Step 1:

Consider the NLPDE of the form

$$F\left(v, v_t, v_x, v_{tt}, v_{xx}, \ldots\ldots\right) = 0. \tag{8}$$

By using the subsequent transformation

$$v\left(x, t\right) = V\left(\eta\right), \eta = x - ct, \tag{9}$$

where $c \neq 0$, we acquire ordinary differential equation (ODE) of the form

$$F\left(v, v', v'', \ldots\ldots\right) = 0 \tag{10}$$

Step 2:

Now, consider the solution of Eq. (8) takes the subsequent form [44,45]

$$V\left(\eta\right) = \sum_{i=0}^{N} a_i a^{if(\eta)}, \tag{11}$$

where a and a_i are constants to be found and $f\left(\eta\right)$ satisfies the DE of the form

$$f'\left(\eta\right) = \frac{1}{\ln a}\left(b_1 a^{-f(\eta)} + b_2 + b_3 a^{f(\eta)}\right). \tag{12}$$

Step 3:

Now, by balancing the nonlinear terms and higher order derivatives in Eq. (10), we find positive integer N.

Step 4:

Utilizing Eqs. (11) and (12) into Eq. (10) and collecting same powers of $a^{if(\eta)}$, where $(i = 0, 1, 2, \ldots)$ and equating to zero, we obtain a system of algebraic equations. To find the values of a^i, β and σ, this system is then solved symbolically. The following are the answers to Eq. (12) related to the coupled cases:

Family 1: If $b_2^2 - b_1 b_3 < 0$ and $b_3 \neq 0$, then

$$a^{f(\eta)} = \frac{-b_2}{b_3} + \frac{\sqrt{-\left(b_2^2 - b_1 b_3\right)}}{b_3} \tan\left(\frac{\sqrt{-\left(b_2^2 - b_1 b_3\right)}}{2}\eta\right), \tag{13}$$

or

$$a^{f(\eta)} = \frac{-b_2}{b_3} + \frac{\sqrt{-\left(b_2^2 - b_1 b_3\right)}}{b_3} \cot\left(\frac{\sqrt{-\left(b_2^2 - b_1 b_3\right)}}{2}\eta\right), \tag{14}$$

Family 2: If $b_2^2 - b_1 b_3 > 0$ and $b_3 \neq 0$, then

$$a^{f(\eta)} = \frac{-b_2}{b_3} - \frac{\sqrt{\left(b_2^2 - b_1 b_3\right)}}{b_3} \tanh\left(\frac{\sqrt{\left(b_2^2 - b_1 b_3\right)}}{2}\eta\right), \tag{15}$$

or

$$a^{f(\eta)} = \frac{-b_2}{b_3} - \frac{\sqrt{\left(b_2^2 - b_1 b_3\right)}}{b_3} \coth\left(\frac{\sqrt{\left(b_2^2 - b_1 b_3\right)}}{2}\eta\right). \tag{16}$$

Family 3: If $b_2^2 + b_1^2 > 0$, $b_3 \neq 0$, and $b_3 = -b_1$, then

$$a^{f(\eta)} = \frac{b_2}{b_3} + \frac{\sqrt{\left(b_2^2 + b_1^2\right)}}{b_3} \tanh\left(\frac{\sqrt{\left(b_2^2 + b_1^2\right)}}{2}\eta\right), \tag{17}$$

or

$$a^{f(\eta)} = \frac{b_2}{b_3} + \frac{\sqrt{\left(b_2^2 + b_1^2\right)}}{b_3} \coth\left(\frac{\sqrt{\left(b_2^2 + b_1^2\right)}}{2}\eta\right). \tag{18}$$

Family 4: If $b_2^2 + b_1^2 < 0$, $b_3 \neq 0$, and $b_3 = -b_1$, then

$$a^{f(\eta)} = \frac{b_2}{b_3} + \frac{\sqrt{-\left(b_2^2 + b_1^2\right)}}{b_1} \tan\left(\frac{\sqrt{-\left(b_2^2 + b_1^2\right)}}{2}\eta\right), \tag{19}$$

or

$$a^{f(\eta)} = \frac{b_2}{b_3} + \frac{\sqrt{-\left(b_2^2 + b_1^2\right)}}{b_1} \cot\left(\frac{\sqrt{-\left(b_2^2 + b_1^2\right)}}{2}\eta\right). \tag{20}$$

Family 5: If $b_2^2 - b_1^2 < 0$, $b_3 \neq 0$, and $b_3 = -b_1$, then

$$a^{f(\eta)} = -\frac{b_2}{b_3} + \frac{\sqrt{\left(b_2^2 + b_1^2\right)}}{b_1} \tan\left(\frac{\sqrt{-\left(b_2^2 + b_1^2\right)}}{2}\eta\right), \tag{21}$$

or

$$a^{f(\eta)} = -\frac{b_2}{b_3} + \frac{\sqrt{\left(b_2^2 + b_1^2\right)}}{b_1} \cot\left(\frac{\sqrt{-\left(b_2^2 + b_1^2\right)}}{2}\eta\right). \tag{22}$$

Family 6: If $b_2^2 - b_1^2 > 0$, $b_3 \neq 0$, and $b_3 = -b_1$, then

$$a^{f(\eta)} = \frac{-b_2}{b_3} + \frac{\sqrt{\left(b_2^2 - b_1^2\right)}}{b_1} \tanh\left(\frac{\sqrt{\left(b_2^2 - b_1^2\right)}}{2}\eta\right), \tag{23}$$

or

$$a^{f(\eta)} = \frac{-b_2}{b_3} + \frac{\sqrt{\left(b_2^2 - b_1^2\right)}}{b_1} \coth\left(\frac{\sqrt{\left(b_2^2 - b_1^2\right)}}{2}\eta\right). \tag{24}$$

Family 7: If $b_1b_3 < 0$, $b_3 \neq 0$, and $b_2 = 0$, then

$$a^{f(\eta)} = \frac{\sqrt{-b_1}}{b_3}\tanh\left(\frac{\sqrt{-b_1b_3}}{2}\eta\right), \tag{25}$$

or

$$a^{f(\eta)} = \frac{\sqrt{-b_1}}{b_3}\coth\left(\frac{\sqrt{-b_1b_3}}{2}\eta\right). \tag{26}$$

Family 8: If $b_2 = 0$, and $b_1 = -b_3$, then

$$a^{f(\eta)} = \frac{-\left(1+e^{2b_1\eta}\right) \pm \sqrt{2\left(e^{4b_1\eta}+1\right)}}{e^{2b_1\eta}-1}, \tag{27}$$

or

$$a^{f(\eta)} = \frac{-\left(1+e^{2b_1\eta}\right) \pm \sqrt{e^{4b_1\eta}+6e^{2b_1\eta}+1}}{2e^{2b_1\eta}}. \tag{28}$$

Family 9: If $b_1 = b_3 = 0$, then

$$a^{f(\eta)} = \frac{-\left(1+e^{2b_2\eta}\right) \pm \sqrt{2\left(e^{4b_2\eta}+1\right)}}{e^{2b_2\eta}-1}, \tag{29}$$

or

$$a^{f(\eta)} = \frac{-\left(1+e^{2b_2\eta}\right) \pm \sqrt{e^{4b_2\eta}+6e^{2b_2\eta}+1}}{2e^{2b_2\eta}}. \tag{30}$$

Family 10: If $b_2^2 = b_1b_3$, then

$$a^{f(\eta)} = \frac{-b_1\left(b_2\eta+2\right)}{b_2^2\eta}. \tag{31}$$

Family 11: If $b_2 = k,\ b_1 = 2k,\ b_3 = 0$, then

$$a^{f(\eta)} = e^{k\eta} - 1. \tag{32}$$

Family 12: If $b_2 = k,\ b_3 = 2k,\ b_1 = 0$, then

$$a^{f(\eta)} = \frac{e^{k\eta}}{1-e^{k\eta}}. \tag{33}$$

Family 13: If $2b_2 = b_1 + b_3$, then

$$a^{f(\eta)} = \frac{1-b_1e^{\frac{1}{2}\left(b_1-b_3\right)\eta}}{1-b_3e^{\frac{1}{2}\left(b_1-b_3\right)\eta}}, \tag{34}$$

or

$$a^{f(\eta)} = \frac{b_1e^{\frac{1}{2}\left(b_1-b_3\right)\eta}+1}{-b_3e^{\frac{1}{2}\left(b_1-b_3\right)\eta}-1}. \tag{35}$$

Family 14: If $-2b_2 = b_1 + b_3$, then

$$a^{f(\eta)} = \frac{e^{\frac{1}{2}(b_1-b_3)\eta} + b_1}{e^{\frac{1}{2}(b_1-b_3)\eta} + b_3}. \tag{36}$$

Family 15: If $b_1 = 0$, then

$$a^{f(\eta)} = \frac{b_2 e^{b_2 b_3}}{1 + \frac{b_3}{2} e^{b_2 b_3}}. \tag{37}$$

Family 16: If $b_2 = b_1 = b_3 \neq 0$, then

$$a^{f(\eta)} = \frac{-(b_1\eta + 2)}{b_1\eta}. \tag{38}$$

Family 17: If $b_2 = b_3 = 0$, then

$$a^{f(\eta)} = \frac{b_1}{2}\eta. \tag{39}$$

Family 18: If $b_2 = b_1 = 0$, then

$$a^{f(\eta)} = -\frac{2}{b_3\eta}. \tag{40}$$

Family 19: If $b_2 = 0$, and $b_1 = b_3$, then

$$a^{f(\eta)} = \tan\left(\frac{b_1\eta + C}{2}\right). \tag{41}$$

Family 20: If $b_2 = 0$, then

$$a^{f(\eta)} = e^{b_2\eta} - \frac{b_1}{2b_2}. \tag{42}$$

3.2 *The Jacobi Elliptic Function Expansion Method*

Step 1: Consider the Eqs. (8) to (10).

Step 2: Now, consider the analytical solution of Eq. (10) takes the following form

$$(F')^2(\eta) = AF^4(\eta) + BF^2(\eta) + C, \tag{43}$$

where $F' = \frac{dF}{d\eta}$, $\eta = \eta(x,t)$ and A, B, C are constants. Table 1 contains the solution to Eq. (43), where $i^2 = -1$.

Table 1: The solution of $F(\eta)$ to Eq. (43) for selected values of A, B, and C [46]

No.	A	B	C	F
1	Ξ^2	$-(1+\Xi^2)$	1	$sn(\eta)$ or $cd(\eta)$
2	$-\Xi^2$	$2\Xi^2-1$	$1-\Xi^2$	$cn(\eta)$
3	-1	$2-\Xi^2$	Ξ^2-1	$dn(\eta)$
4	1	$-(1+\Xi^2)$	Ξ^2	$ns(\eta)$ or $dc(\eta)$
5	$1-\Xi^2$	$2\Xi^2-1$	$-\Xi^2$	$nc(\eta)$
6	Ξ^2-1	$2-\Xi^2$	-1	$nd(\eta)$
7	$1-\Xi^2$	$2-\Xi^2$	1	$sc(\eta)$
8	$-\Xi^2(1-\Xi^2)$	$2-\Xi^2-1$	1	$sd(\eta)$
9	1	$2-\Xi^2$	$1-\Xi^2$	$cs(\eta)$
10	1	$2\Xi^2-1$	$-\Xi^2\left(1-\Xi^2\right)$	$ds(\eta)$
11	$\frac{-1}{4}$	$\frac{\Xi^2+1}{2}$	$-\frac{\left(1-\Xi^2\right)^2}{4}$	$rcn(\eta) \mp dn(\eta)$
12	$\frac{1}{4}$	$\frac{-2\Xi^2+1}{2}$	$\frac{1}{4}$	$ns(\eta) \mp cs(\eta)$
13	$\frac{1-\Xi^2}{4}$	$\frac{\Xi^2+1}{2}$	$\frac{1-\Xi^2}{4}$	$nc(\eta) \mp sc(\eta)$
14	$\frac{1}{4}$	$\frac{\Xi^2-2}{2}$	$\frac{\Xi^4}{4}$	$ns(\eta) \mp ds(\eta)$
15	$\frac{\Xi^2}{4}$	$\frac{\Xi^2-2}{2}$	$\frac{\Xi^4}{4}$	$sn(\eta) \mp icn(\eta)\,,\ \frac{dn(\eta)}{\sqrt{1-r^2 sn(\eta)} \mp cn(\eta)}$
16	$\frac{1}{4}$	$\frac{1-2\Xi^2}{2}$	$\frac{1}{4}$	$rcn(\eta) \mp idn(\eta)\,,\ \frac{sn(\eta)}{1 \mp cn(\eta)}$
17	$\frac{\Xi^2}{4}$	$\frac{\Xi^2-2}{2}$	$\frac{1}{4}$	$\frac{sn(\eta)}{1 \mp dn(\eta)}$
18	$\frac{\Xi^2-1}{4}$	$\frac{\Xi^2+2}{2}$	$\frac{\Xi^2-1}{4}$	$\frac{dn(\eta)}{1 \mp rsn(\eta)}$
19	$\frac{1-\Xi^2}{4}$	$\frac{\Xi^2+1}{2}$	$\frac{-\Xi^2+1}{4}$	$\frac{cn(\eta)}{1 \mp sn(\eta)}$
20	$\frac{\left(1-\Xi^2\right)^2}{4}$	$\frac{\Xi^2+1}{2}$	$\frac{1}{4}$	$\frac{sn(\eta)}{dn(\eta) \mp cn(\eta)}$
21	$\frac{\Xi^4}{4}$	$\frac{\Xi^2-2}{2}$	$\frac{1}{4}$	$\frac{cn(\eta)}{\sqrt{1-r^2 \mp dn(\eta)}}$

The Jacobian elliptic functions (JEFs) $sn(\eta) = sn(\eta;\Xi)$, $cn(\eta) = cn(\eta;\Xi)$ and $dn(\eta) = dn(\eta;\Xi)$, where Ξ $(0 < \Xi < 1)$ is the modulus, satisfies the subsequent properties:

$$\begin{cases} sn^2(\eta) + cn^2(\eta) = 1, \\ dn^2(\eta) + \Xi sn^2(\eta) = 1, \\ \dfrac{d}{d\eta} sn(\eta) = cn(\eta)\, dn(\eta), \\ \dfrac{d}{d\eta} cn(\eta) = -sn(\eta)\, dn(\eta), \\ \dfrac{d}{d\eta} dn(\eta) = -\Xi^2 cn(\eta)\, sn(\eta). \end{cases}$$

Since $\Xi \to 0$ and $\Xi \to 1$ JEFs, which are presented in Table 2, turns into trigonometric and hyperbolic functions. Consequently, we get several solutions for the equation under consideration.

Table 2: The JEFs for $\Xi \to 1$ and $\Xi \to 0$ [46]

Function	$\Xi \to 1$	$\Xi \to 0$	Function	$\Xi \to 1$	$\Xi \to 0$
$sn(v)$	$\tanh(v)$	$\sin(v)$	$ns(v)$	$\coth(v)$	$\csc(v)$
$cd(v)$	1	$\cos(v)$	$dc(v)$	1	$\sec(v)$
$cn(v)$	$\text{sech}(v)$	$\cos(v)$	$nc(v)$	$\cosh(v)$	$\sec(v)$
$dn(v)$	$\text{sech}(v)$	1	$nd(v)$	$\cosh(v)$	1
$sc(v)$	$\sinh(v)$	$\tan(v)$	$cs(v)$	$\text{csch}(v)$	$\cot(v)$
$sd(v)$	$\sinh(v)$	$\sin(v)$	$ds(v)$	$\text{csch}(v)$	$\csc(v)$

A finite sequence of JEFs can be used to represent $v(\eta)$ using the JEFM

$$v(\eta) = \sum_{i=0}^{N} a_i F^i(\eta), \tag{44}$$

where $F(\eta)$ is the solution of the Eq. (43) and k, a_i $(i = 0, 1, 2, ..., k)$ are constants. By utilizing the balancing principle technique in Eq. (10), k can be determined. A system of algebraic equations for is produced by substituting Eqs. (44) into (10) and setting all of the coefficients of power of F to zero. Then, we can solve this system by utilizing all the values of Eq. (43) in Table 1.

4 Application of Analytical Techniques

Consider the transformation of the form

$$v(x,t) = V(\eta), \eta = x - ct. \tag{45}$$

We derive the subsequent ODE by utilizing Eqs. (45) into (7).

$$c^2 V'' - \{\left[\left(d_0^2 + pV + qV^2\right) V'\right]' - k_1 V^{(4)} + c^2 k_2 V^{(4)} = 0. \tag{46}$$

Now, we get the subsequent nonlinear ordinary differential equation by setting the integration constant to zero for convenience. The subsequent ODE is obtained by integrating Eq. (45) twice with respect to η and for convenience setting the integration constant equal to zero.

$$6\left(c^2k_2 - k_1\right)V'' + 3pV^2 + 2qV^3 + 6\left(c - d_0^2\right) = 0. \tag{47}$$

4.1 Application of Khater Method

The general solution of Khater method is given as

$$V(\eta) = \sum_{i=0}^{N} a_i a^{if(\eta)}, \tag{48}$$

We acquire $N = 1$ by applying the homogeneous balancing method (HBM) between v^3 and v'' in Eq. (47). For $N = 1$, we have

$$V(\eta) = a_0 + a_1 a^{f(\eta)}, \tag{49}$$

where a_0, a_1 are constants and $a_1 \neq 0$. By substituting Eqs. (49) into (48) and incorporating Eq. (12), we equate the coefficients of the same power $a^{if(\eta)}$ to zero, thereby establishing a system of algebraic equations. Following symbolic computation, we resolve the system of equations, leading to the subsequent cases along with their corresponding solutions.

$$a_0 = \Delta, a_1 = \Delta_1, c = \frac{\sqrt{-p^3 + 12d_0^2q^2}}{2\sqrt{3}q}, k_2 = \frac{6\left(p^2q - 2k_1q^2\beta^2 + 8k_1q^2\alpha\sigma\right)}{\left(p^3 - 12d_0^2q^2\right)\left(\beta^2 - 4\alpha\sigma\right)},$$

where

$$\Delta = \frac{pq\beta^2 - 4pq\alpha\sigma - \sqrt{3}\sqrt{p^2q^2\beta^4 - 4p^2q^2\alpha\beta^2\sigma}}{2\left(-q^2\beta^2 + 4q^2\alpha\sigma\right)},$$

$$\Delta_1 = \frac{p\sigma + \dfrac{pq^2\beta^2\sigma}{-q^2\beta^2 + 4q^2\alpha\sigma} - \dfrac{4pq^2\alpha\sigma^2}{-q^2\beta^2 + 4q^2\alpha\sigma} - \dfrac{\sqrt{3}q\sigma\sqrt{p^2q^2\beta^2\left(\beta^2 - 4\alpha\sigma\right)}}{-q^2\beta^2 + 4q^2\alpha\sigma}}{q\beta}.$$

This results in the subsequent solution, based on the corresponding cases.

Family 1: If $b_2^2 - b_1b_3 < 0$, $b_3 \neq 0$, then

$$v_1(x,t) = \Delta + \Delta_1\left(\frac{-b_2}{b_3} + \frac{\sqrt{-\left(b_2^2 - b_1b_3\right)}}{b_3}\tan\left(\frac{\sqrt{-\left(b_2^2 - b_1b_3\right)}}{2}\eta\right)\right), \tag{50}$$

or

$$v_2(x,t) = \Delta + \Delta_1\left(\frac{-b_2}{b_3} + \frac{\sqrt{-\left(b_2^2 - b_1b_3\right)}}{b_3}\cot\left(\frac{\sqrt{-\left(b_2^2 - b_1b_3\right)}}{2}\eta\right)\right). \tag{51}$$

Family 2: If $b_2^2 - b_1b_3 > 0$, $b_3 \neq 0$, then

$$v_4(x,t) = \Delta + \Delta_1\left(\frac{-b_2}{b_3} - \frac{\sqrt{\left(b_2^2 - \alpha b_3\right)}}{b_3}\tanh\left(\frac{\sqrt{\left(b_2^2 - b_1b_3\right)}}{2}\eta\right)\right), \tag{52}$$

or

$$v_4(x,t) = \Delta + \Delta_1 \left(\frac{-b_2}{b_3} - \frac{\sqrt{\left(b_2^2 - \alpha b_3\right)}}{b_3} \coth\left(\frac{\sqrt{\left(b_2^2 - b_1 b_3\right)}}{2} \eta \right) \right). \tag{53}$$

Family 3: If $b_1^2 + b_2^2 > 0$, $b_3 \neq 0$, and $b_3 = -b_1$, then

$$v_5(x,t) = \Delta + \Delta_1 \left(\frac{b_2}{b_3} + \frac{\sqrt{\left(b_2^2 + b_1^2\right)}}{b_1} \tanh\left(\frac{\sqrt{\left(b_2^2 + b_1^2\right)}}{2} \eta \right) \right), \tag{54}$$

or

$$v_6(x,t) = \Delta + \Delta_1 \left(\frac{b_2}{b_3} + \frac{\sqrt{\left(b_2^2 + b_1^2\right)}}{b_1} \coth\left(\frac{\sqrt{\left(b_2^2 + b_1^2\right)}}{2} \eta \right) \right). \tag{55}$$

Family 4: If $b_2^2 + b_1^2 < 0$, $b_3 \neq 0$ and $b_3 = -b_1$, then

$$v_7(x,t) = \Delta + \Delta_1 \left(\frac{b_2}{b_3} + \frac{\sqrt{-\left(b_2^2 + b_1^2\right)}}{b_1} \tan\left(\frac{\sqrt{-\left(b_2^2 + b_1^2\right)}}{2} \eta \right) \right), \tag{56}$$

or

$$v_8(x,t) = \Delta + \Delta_1 \left(\frac{b_2}{b_3} + \frac{\sqrt{-\left(b_2^2 + b_1^2\right)}}{b_1} \cot\left(\frac{\sqrt{-\left(b_2^2 + b_1^2\right)}}{2} \eta \right) \right). \tag{57}$$

Family 5: If $b_2^2 - b_1^2 < 0$, $b_3 \neq 0$, and $b_3 = b_1$, then

$$v_9(x,t) = \Delta + \Delta_1 \left(\frac{-b_1}{b_3} + \frac{\sqrt{-\left(b_2^2 - b_1^2\right)}}{b_1} \tan\left(\frac{\sqrt{-\left(b_2^2 - b_1^2\right)}}{2} \eta \right) \right), \tag{58}$$

or

$$v_{10}(x,t) = \Delta + \Delta_1 \left(\frac{-b_1}{b_3} + \frac{\sqrt{-\left(b_2^2 - b_1^2\right)}}{b_1} \cot\left(\frac{\sqrt{-\left(b_2^2 - b_1^2\right)}}{2} \eta \right) \right). \tag{59}$$

Family 6: If $b_2^2 - b_1^2 > 0$, $b_3 \neq 0$, *and* $b_3 = b_1$, then

$$v_{11}(x,t) = \Delta + \Delta_1 \left(\frac{-b_2}{b_3} + \frac{\sqrt{\left(b_2^2 - b_1^2\right)}}{b_1} \tanh\left(\frac{\sqrt{\left(b_2^2 - b_1^2\right)}}{2} \eta \right) \right), \tag{60}$$

or

$$v_{12}(x,t) = \Delta + \Delta_1 \left(\frac{-b_2}{b_3} + \frac{\sqrt{\left(b_2^2 - b_1^2\right)}}{b_1} \coth\left(\frac{\sqrt{\left(b_2^2 - b_1^2\right)}}{2} \eta \right) \right). \tag{61}$$

Family 7: If $b_1b_3 < 0$, $b_3 \neq 0$, $b_2 = 0$, then

$$v_{13}(x,t) = \Delta + \Delta_1 \left(\frac{\sqrt{-b_1}}{b_3} \tanh \left(\frac{\sqrt{-b_1 b_3}}{2} \eta \right) \right), \tag{62}$$

or

$$v_{14}(x,t) = \Delta + \Delta_1 \left(\frac{\sqrt{-b_1}}{b_3} \coth \left(\frac{\sqrt{-b_1 b_3}}{2} \eta \right) \right). \tag{63}$$

Family 8: If $b_2 = 0$, $b_1 = -b_3$, then

$$v_{15}(x,t) = \Delta + \Delta_1 \left(\frac{-\left(1 + e^{2b_1\eta}\right) \pm \sqrt{2\left(e^{4b_1\eta} + 1\right)}}{e^{2b_1\eta} - 1} \right), \tag{64}$$

or

$$v_{16}(x,t) = \Delta + \Delta_1 \left(\frac{-\left(1 + e^{2b_1\eta}\right) \pm \sqrt{e^{4b_1\eta} + 6e^{2b_1\eta} + 1}}{2e^{2b_1\eta}} \right). \tag{65}$$

Family 9: If $b_1 = b_3 = 0$, then

$$v_{17}(x,t) = \Delta + \Delta_1 \left(\frac{-\left(1 + e^{2b_2\eta}\right) \pm \sqrt{2\left(e^{4b_2\eta} + 1\right)}}{e^{2b_2\eta} - 1} \right). \tag{66}$$

or

Family 10: If $b_2^2 = b_1 b_3$, then

$$v_{19}(x,t) = \Delta + \Delta_1 \left(\frac{-b_1\left(b_2\eta + 2\right)}{b_2^2\eta} \right). \tag{67}$$

Family 11: If $b_2 = \upsilon$, $b_1 = 2\upsilon$, $b_3 = 0$, then

$$v_{20}(x,t) = \Delta + \Delta_1 \left(e^{\upsilon\eta} - 1\right). \tag{68}$$

Family 12: If $b_2 = \upsilon, b_1 = 2\upsilon, b_1 = 0$, then

$$v_{21}(x,t) = \Delta + \Delta_1 \left(\frac{e^{\upsilon\eta}}{1 - e^{\upsilon\eta}} \right). \tag{69}$$

Family 13: If $2b_2 = b_1 + b_3$, then

$$v_{22}(x,t) = \Delta + \Delta_1 \left(\frac{1 - b_1 e^{\frac{1}{2}\left(b_1 - b_3\right)\eta}}{1 - b_3 e^{\frac{1}{2}\left(b_1 - b_3\right)\eta}} \right), \tag{70}$$

or

$$v_{23}(x,t) = \Delta + \Delta_1 \left(\frac{b_1 e^{\frac{1}{2}\left(b_1 - b_3\right)\eta} + 1}{-b_3 e^{\frac{1}{2}\left(b_1 - b_3\right)\eta} - 1} \right). \tag{71}$$

Family 14: If $-2b_2 = b_1 + b_3$, then

$$v_{24}(x,t) = \Delta + \Delta_1 \left(\frac{e^{\frac{1}{2}(b_1-b_3)\eta} + b_1}{e^{\frac{1}{2}(b_1-b_3)\eta} + b_3} \right). \tag{72}$$

Family 15: If $b_1 = 0$, then

$$v_{25}(x,t) = \Delta + \Delta_1 \left(\frac{b_2 e^{b_2 b_3}}{1 + \frac{b_3}{2} e^{b_2 b_3}} \right). \tag{73}$$

Family 16: If $b_2 = b_1 = b_3 \neq 0$, then

$$v_{26}(x,t) = \Delta + \Delta_1 \left(\frac{-(b_1\eta + 2)}{b_1\eta} \right). \tag{74}$$

Family 17: If $b_2 = b_3 = 0$, then

$$v_{27}(x,t) = \Delta + \Delta_1 \left(\frac{b_1}{2}\eta \right). \tag{75}$$

Family 18: If $b_2 = b_1 = 0$, then

$$v_{28}(x,t) = \Delta + \Delta_1 \left(-\frac{2}{\sigma\eta} \right). \tag{76}$$

Family 19: If $b_2 = 0$, $b_1 = b_3$, then

$$v_{29}(x,t) = \Delta + \Delta_1 \left(\tan\left(\frac{b_1\eta + C}{2} \right) \right). \tag{77}$$

Family 20: If $b_3 = 0$, then

$$v_{30}(x,t) = \Delta + \Delta_1 \left(e^{b_2\eta} - \frac{b_1}{2b_2} \right). \tag{78}$$

4.2 *Application of Jacobi Elliptic Function Expansion Method*

By using the equilibrium rule, Eq. (47) will take the subsequent form

$$v(\eta) = a_0 + a_1 F(\eta), \tag{79}$$

where a_0, a_1 are constants and $a_1 \neq 0$. When Eq. (79) and its necessary derivatives are inserted into Eq. (47), we obtain a polynomial in the form of $F^l(\eta)$. We then equate the powers of $F^l(\eta)$ to zero, producing algebraic equations. We can determine the following values after utilizing computer tools to solve this system of equations.

$$a_0 = -\frac{p}{2q}, a_1 = -\frac{\sqrt{k_2p^3 + 12k_1q^2 - 12d_0^2k_2q^2}}{\sqrt{2}q^{3/2}},$$
$$c = -\frac{\sqrt{-p^3 + 12d_0^2q^2}}{2\sqrt{3}q}, B = -\frac{3p^2q}{k_2p^3 + 12k_1q^2 - 12d_0^2k_2q^2}.$$

We derive the exact solution of Eq. (47) by combining the previously reported solution approach.

When $A = \Xi^2$, $B = -\left(1 + \Xi^2\right)$, $R = 1$, Table 1 provides $F = sn$, so the periodic solution can be represented as

$$v_1 = -\frac{p}{2q} - \frac{\sqrt{k_2 p^3 + 12k_1 q^2 - 12d_0^2 k_2 q^2}}{\sqrt{2} q^{3/2}} \Xi sn\left(\eta\right). \tag{80}$$

If $\Xi \to 1$, from Table 2, the solitary wave solutions (SWS) can de derived as

$$v_2 = -\frac{p}{2q} - \frac{\sqrt{k_2 p^3 + 12k_1 q^2 - 12d_0^2 k_2 q^2}}{\sqrt{2} q^{3/2}} \tanh\left(\eta\right). \tag{81}$$

When $A = -\Xi^2$, $B = 2\Xi^2 - 1$, $R = 1 - \Xi^2$, Table 1 provides $F = cn$, so the periodic solution can be represented as

$$v_3 = -\frac{p}{2q} - \frac{\sqrt{k_2 p^3 + 12k_1 q^2 - 12d_0^2 k_2 q^2}}{\sqrt{2} q^{3/2}} \Xi cn\left(\eta\right). \tag{82}$$

If $\Xi \to 1$, from Table 2, the SWS can de derived as

$$v_4 = -\frac{p}{2q} - \frac{\sqrt{k_2 p^3 + 12k_1 q^2 - 12d_0^2 k_2 q^2}}{\sqrt{2} q^{3/2}} \operatorname{sech}(\eta). \tag{83}$$

When $A = -1$, $B = 2 - \Xi^2$, $R = \Xi^2 - 1$, Table 1 provides $F = dn$, so the periodic solution can be represented as

$$v_5 = -\frac{p}{2q} - \frac{\sqrt{k_2 p^3 + 12k_1 q^2 - 12d_0^2 k_2 q^2}}{\sqrt{2} q^{3/2}} sn\left(\eta\right). \tag{84}$$

It is evident from Table 2 that this solution for $\Xi \to 1$ is comparable to the single solution of Eq. (83).

When $A = 1$, $B = -(1 + \Xi^2)$, $R = \Xi^2$, Table 1 provides $F = ns$, so the periodic solution can be represented as

$$v_6 = -\frac{p}{2q} - \frac{\sqrt{k_2 p^3 + 12k_1 q^2 - 12d_0^2 k_2 q^2}}{\sqrt{2} q^{3/2}} ns\left(\eta\right). \tag{85}$$

If $\Xi \to 1$, from Table 2, the SWS can de derived as

$$v_7 = -\frac{p}{2q} - \frac{\sqrt{k_2 p^3 + 12k_1 q^2 - 12d_0^2 k_2 q^2}}{\sqrt{2} q^{3/2}} \coth\left(\eta\right). \tag{86}$$

When $A = 1$, $B = -(1 + \Xi^2)$, $R = \Xi^2$, Table 1 provides $F = dc$, so the periodic solution can be represented as

$$v_8 = -\frac{p}{2q} - \frac{\sqrt{k_2 p^3 + 12k_1 q^2 - 12d_0^2 k_2 q^2}}{\sqrt{2} q^{3/2}} dc\left(\eta\right). \tag{87}$$

When $A = 1 - \Xi^2$, $B = 2\Xi^2 - 1$, $R = -\Xi^2$, Table 1 provides $F = nc$, so the periodic solution can be represented as

$$v_9 = -\frac{p}{2q} - \frac{\sqrt{k_2 p^3 + 12k_1 q^2 - 12d_0^2 k_2 q^2}}{\sqrt{2} q^{3/2}} nc\left(\eta\right). \tag{88}$$

If $\Xi \to 0$, from Table 2, the SWS can de derived as

$$v_{10} = -\frac{p}{2q} - \frac{\sqrt{k_2 p^3 + 12k_1 q^2 - 12d_0^2 k_2 q^2}}{\sqrt{2} q^{3/2}} \sec\left(\eta\right). \tag{89}$$

When $A = 1 - \Xi^2$, $B = 2 - \Xi^2$, $R = 1$, Table 1 provides $F = sc$, so the periodic solution can be represented as

$$v_{11} = -\frac{p}{2q} - \frac{\sqrt{k_2 p^3 + 12k_1 q^2 - 12d_0^2 k_2 q^2}}{\sqrt{2} q^{3/2}} sc\left(\eta\right). \tag{90}$$

If $\Xi \to 0$, from Table 2, the periodic solution can de derived as

$$v_{12} = -\frac{p}{2q} - \frac{\sqrt{k_2 p^3 + 12k_1 q^2 - 12d_0^2 k_2 q^2}}{\sqrt{2} q^{3/2}} \tan\left(\eta\right). \tag{91}$$

When $A = 1$, $B = 2 - \Xi^2$, $R = 1 - \Xi^2$, Table 1 provides $F = cs$, so the periodic solution can be represented as

$$v_{13} = -\frac{p}{2q} - \frac{\sqrt{k_2 p^3 + 12k_1 q^2 - 12d_0^2 k_2 q^2}}{\sqrt{2} q^{3/2}} cs\left(\eta\right). \tag{92}$$

If $\Xi \to 1$, from Table 2, the SWS can de derived as

$$v_{14} = -\frac{p}{2q} - \frac{\sqrt{k_2 p^3 + 12k_1 q^2 - 12d_0^2 k_2 q^2}}{\sqrt{2} q^{3/2}} \operatorname{csch}\left(\eta\right). \tag{93}$$

If $\Xi \to 0$, from Table 2, the SWS can de derived as

$$v_{15} = -\frac{p}{2q} - \frac{\sqrt{k_2 p^3 + 12k_1 q^2 - 12d_0^2 k_2 q^2}}{\sqrt{2} q^{3/2}} \cot\left(\eta\right). \tag{94}$$

When $A = 1$, $B = 2\Xi^2 - 1$, $R = \Xi^4 - \Xi^2$, Table 1 provides $F = ds$, so the periodic solution can be represented as

$$v_{16} = -\frac{p}{2q} - \frac{\sqrt{k_2 p^3 + 12k_1 q^2 - 12d_0^2 k_2 q^2}}{\sqrt{2} q^{3/2}} ds\left(\eta\right). \tag{95}$$

When $A = -\frac{1}{4}$, $B = \frac{\Xi^2+1}{2}$, $R = \frac{-(1+\Xi^2)}{4}$, Table 1 provides $F = \Xi cn \mp dn$, so the periodic solution can be represented as

$$v_{17} = -\frac{p}{2q} - \frac{\sqrt{k_2 p^3 + 12k_1 q^2 - 12d_0^2 k_2 q^2}}{\sqrt{2} q^{3/2}} \Xi cn(\eta) \mp dn(\eta). \tag{96}$$

If $\Xi \to 0$, the solution is same as Eq. (81).

When $A = \frac{1}{4}$, $B = \frac{\Xi^2+1}{2}$, $R = \frac{1}{4}$, Table 1 provides $F = \Xi ns \mp cs$, so the periodic solution can be represented as

$$v_{18} = -\frac{p}{2q} - \frac{\sqrt{k_2p^3 + 12k_1q^2 - 12d_0^2k_2q^2}}{\sqrt{2}q^{3/2}}ns(\eta) \mp cs(\eta). \tag{97}$$

When $A = \frac{1-\Xi^2}{4}$, $B = \frac{\Xi^2+1}{2}$, $R = \frac{1-\Xi^2}{4}$, Table 1 provides $F = \Xi nc \mp sc$, so the periodic solution can be represented as

$$v_{19} = -\frac{p}{2q} - \frac{\sqrt{k_2p^3 + 12k_1q^2 - 12d_0^2k_2q^2}}{\sqrt{2}q^{3/2}}\Xi nc(\eta) \mp sc(\eta). \tag{98}$$

If $\Xi \to 0$, the solution can be derived as

$$v_{20} = -\frac{p}{2q} - \frac{\sqrt{k_2p^3 + 12k_1q^2 - 12d_0^2k_2q^2}}{\sqrt{2}q^{3/2}} \sec(\eta) \mp \tan(\eta). \tag{99}$$

When $A = \frac{\Xi^2}{4}$, $B = \frac{\Xi^2-2}{2}$, $R = \frac{\Xi^2}{4}$, Table 1 provides $F = sn \mp icn$, so the periodic solution can be represented as

$$v_{21} = -\frac{p}{2q} - \frac{\sqrt{k_2p^3 + 12k_1q^2 - 12d_0^2k_2q^2}}{\sqrt{2}q^{3/2}}sn(\eta) \mp icn(\eta). \tag{100}$$

If $\Xi \to 1$, the solution can be derived as

$$v_{22} = -\frac{p}{2q} - \frac{\sqrt{k_2p^3 + 12k_1q^2 - 12d_0^2k_2q^2}}{\sqrt{2}q^{3/2}} \tanh(\eta) \mp i\mathrm{sech}(\eta). \tag{101}$$

When $A = \frac{1}{4}$, $B = \frac{1-\Xi^2}{2}$, $R = \frac{1}{4}$, Table 1 provides $F = \Xi msn \mp idn$, so the periodic solution can be represented as

$$v_{23} = -\frac{p}{2q} - \frac{\sqrt{k_2p^3 + 12k_1q^2 - 12d_0^2k_2q^2}}{\sqrt{2}q^{3/2}}\Xi sn(\eta) \mp idn(\eta). \tag{102}$$

If $\Xi \to 1$, the solution is same as Eq. (101). When $A = \frac{1}{4}$, $B = \frac{1-\Xi^2}{2}$, $R = \frac{1}{4}$, Table 1 provides $F = \frac{sn(\eta)}{1 \mp cn(\eta)}$, so the periodic solution can be represented as

$$v_{24} = -\frac{p}{2q} - \frac{\sqrt{k_2p^3 + 12k_1q^2 - 12d_0^2k_2q^2}}{\sqrt{2}q^{3/2}} \left(\frac{sn(\eta)}{1 \mp cn(\eta)}\right). \tag{103}$$

If $\Xi \to 1$, the solution can be derived as

$$v_{25} = -\frac{p}{2q} - \frac{\sqrt{k_2p^3 + 12k_1q^2 - 12d_0^2k_2q^2}}{\sqrt{2}q^{3/2}} \left(\frac{\tanh(\eta)}{1 \mp \mathrm{sech}(\eta)}\right). \tag{104}$$

When $A = \frac{\Xi^2}{4}, B = \frac{\Xi^2-2}{2}, R = \frac{\Xi^2}{4}$, Table 1 provides $F = \frac{cn(\eta)}{1 \mp sn(\eta)}$, so the periodic solution can be represented as

$$v_{26} = -\frac{p}{2q} - \frac{\sqrt{k_2 p^3 + 12k_1 q^2 - 12d_0^2 k_2 q^2}}{\sqrt{2} q^{3/2}} \left(\frac{sn(\eta)}{1 \mp dn(\eta)} \right). \tag{105}$$

If $\Xi \to 1$, the solution can be derived

$$v_{27} = -\frac{p}{2q} - \frac{\sqrt{k_2 p^3 + 12k_1 q^2 - 12d_0^2 k_2 q^2}}{\sqrt{2} q^{3/2}} \left(\frac{\sin(\eta)}{1 \mp \cos(\eta)} \right). \tag{106}$$

When $A = \frac{1-\Xi^2}{4}$, $B = \frac{\Xi^2+1}{2}$, $R = \frac{1-\Xi^2}{4}$, Table 1 provides $F = \frac{cn(\eta)}{1 \mp sn(\eta)}$, so the periodic solution can be represented as

$$v_{28} = -\frac{p}{2q} - \frac{\sqrt{k_2 p^3 + 12k_1 q^2 - 12d_0^2 k_2 q^2}}{\sqrt{2} q^{3/2}} \left(\frac{cn(\eta)}{1 \mp cn(\eta)} \right). \tag{107}$$

When $A = \frac{(1-\Xi^2)^2}{4}$, $B = \frac{\Xi^2+1}{2}$, $R = \frac{1}{4}$, Table 1 provides $F = \frac{sn(\eta)}{dn(\eta) \mp cn(\eta)}$, so the solution can be represented as

$$v_{29} = -\frac{p}{2q} - \frac{\sqrt{k_2 p^3 + 12k_1 q^2 - 12d_0^2 k_2 q^2}}{\sqrt{2} q^{3/2}} \left(\frac{sn(\eta)}{dn \mp \cos(\eta)} \right). \tag{108}$$

If $\Xi \to 1$, the solution is same as Eq. (104).

5 Results and Discussion

The acquired results are visually represented through simulations to provide insights into both their qualitative and quantitative characteristics, as well as to demonstrate the dynamic behavior of the primary equations. To maintain precision and clarity, each solution is graphically illustrated in accordance with the relevant parametric parameters. To produce clearly defined analytical expressions and visually appealing graphs that accurately represent the dynamics of the solutions, the constants within the equation are meticulously selected. The analytical solutions obtained through the Khater method and the JEF method demonstrate a wide range of solitary wave structures. These results highlight the strength and adaptability of the methods used in accurately representing intricate wave dynamics within the BTE. The Khater method yields solutions that display stable soliton structures, maintain their shape over time. This stability is essential for applications in optical communications, where maintaining signal integrity over extended distances is critical. Solutions generated by the Khater method exhibit unique propagation characteristics, underscoring the influence of various analytical techniques on wave dynamics. These variations accentuate the method's capability to produce a variety of wave profiles that are appropriate for different physical contexts. The JEF method provides thorough solutions that encompass the three-dimensional structure and phase dynamics of the wave function. The flexibility of this method is apparent in its capacity to articulate complex wave interactions and stability attributes. The implementation of these methods in the BTE presents numerous important advancements in the discipline. The research confirms the effectiveness of sophisticated techniques in addressing intricate nonlinear systems, delivering precise solutions that deepen our comprehension of wave dynamics. This significantly contributes by providing innovative analytical instruments for multi-component wave interactions.

Fig. 2 depicts the analytical solution of Eq. (52), which is anti-kink soliton for $b_2 = 5, b_1 = 2, b_3 = 3, p = 0.5, q = 5, d_0 = 1$. Fig. 3 shows the analytical solution of Eq. (54), which is kink soliton for $b_2 = 5, b_1 = -2, b_3 = 2, p = 0.5, q = 5, d_0 = 1$. Fig. 4 represents the analytical solution of Eq. (60), which is kink soliton for $b_2 = 3, b_1 = 2, b_3 = 2, p = -0.5, q = 0.5, d_0 = 2$. Figs. 5 and 6 show periodic soliton solution for Eq. (79) by considering $p = -3.5, q = -3, k_1 = 2, k_2 = 0.9, d_0 = 1.5, \Xi = 0.5$, and $p = -3.5, q = -3, k_1 = -2, k_2 = 0.9, d_0 = 1.5, \Xi = 0.5$, respectively. Fig. 7 represents the analytical solution of Eq. (80), which is dark soliton for $p = -3.5, q = -3, k_1 = -2, k_2 = 0.9, d_0 = 1.5, \Xi = 0.5$. Figs. 8 and 9 show periodic soliton solution for Eq. (81) by considering $p = 0.9, q = 0.3, k_1 = -2, k_2 = 0.9, d_0 = 1.5, \Xi = 0.5$, and $p = 0.9, q = 0.3, k_1 = -2, k_2 = 0.9, d_0 = 1.5, \Xi = 0.5$, respectively. Fig. 10 represents the analytical solution of Eq. (82), which is dark soliton for $p = 0.9, q = 0.3, k_1 = -2, k_2 = 0.9, d_0 = 1.5$. Fig. 11 represents the analytical solution of Eq. (82), which is bright soliton for $p = 0.9, q = 0.3, k_1 = -2, k_2 = 0.9, d_0 = 1.5$. Fig. 12 represents the analytical solution of Eq. (83), which is periodic soliton for $p = 0.9, q = 0.3, k_1 = 0.2, k_2 = 0.9, d_0 = 1.5$. Fig. 13 represents the analytical solution of Eq. (92), which is bright soliton with high amplitude for $p = 2.9, q = 0.3, k_1 = -2, k_2 = 6, d_0 = 1.5$. Fig. 14 represents the analytical solution of Eq. (95), which is periodic soliton for $p = 2.9, q = 0.3, k_1 = -2, k_2 = 0.6, d_0 = 1.5, \Xi = 0.5$. Figs. 15 and 16 represent analytical solution of Eqs. (100) and (103) which is dark soliton by considering $p = -0.9, q = 0.3, k_1 = 0.2, k_2 = 0.6, d_0 = 1.5$, and $p = -0.9, q = 0.3, k_1 = 0.2, k_2 = 0.6, d_0 = 1.5$, respectively. The soliton solutions represented in this paper provide unprecedented insight into the wave characteristics of biomembranes. The kink, anti-kink, bright, dark, and periodic soliton solutions are very closely related to the mechanical pulses of a continuing experimental to be demonstrated along nerve membranes. For example, the bright soliton is purposely modeled on the localized compression of the lipid bilayer, while the kink solutions are used to model the step like transitions of the density of membrane. These solitons represent traveling mechanical signals that conform to the Heimburg - Jackson model of nerve pulse propagation and provide an alternative to purely electrical models. As such, the waveforms derived from this paper are both mathematically novel and biologically relevant with possible applications in modeling nerve signal transmission neuromechanics, and soft-matter biophysics.

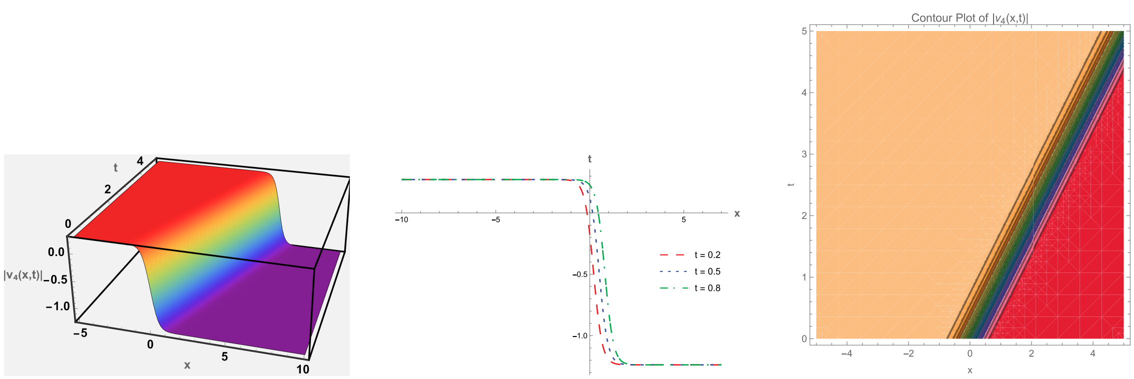

(a) 3D plot (b) contour plot (c) 2D plot

Figure 2: The wave profile representing anti-kink soliton solution for Eq. (52), (a) 3D plot (b) Contour plot (c) 2D plot, when $b_2 = 5,\ b_1 = 2,\ b_3 = 3,\ p = 0.5,\ q = 5,\ d_0 = 1$

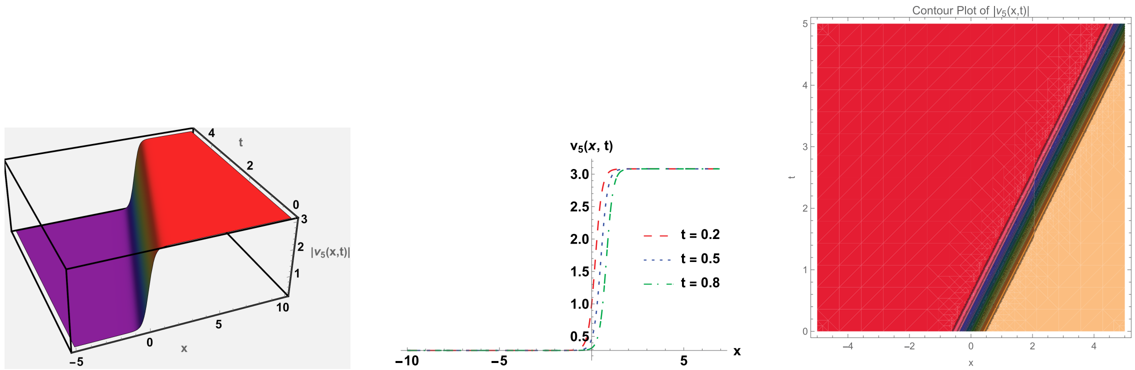

(a) 3D plot (b) contour plot (c) 2D plot

Figure 3: The wave profile kink soliton solution for Eq. (54), (a) 3D plot (b) Contour plot (c) 2D plot, when $b_2 = 5,\ b_1 = -2,\ b_3 = 2,\ p = 0.5,\ q = 5,\ d_0 = 1$

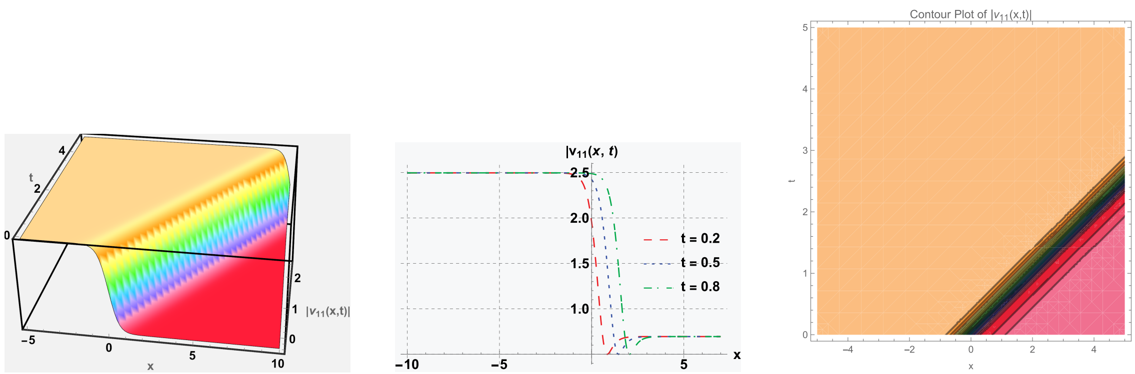

(a) 3D plot (b) contour plot (c) 2D plot

Figure 4: The wave profile representing anti-kink soliton solution for Eq. (60), (a) 3D plot (b) Contour plot (c) 2D plot, when $b_2 = 3,\ b_1 = 2,\ b_3 = 2,\ p = -0.5,\ q = 0.5,\ d_0 = 2$

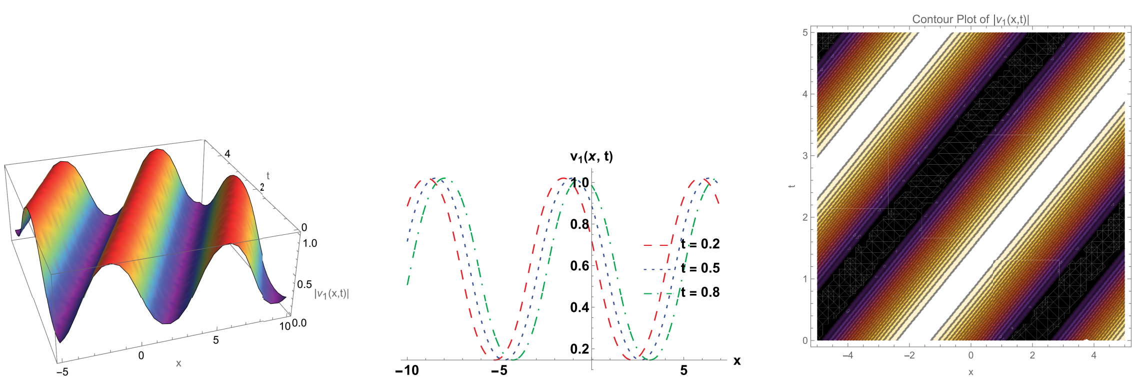

(a) 3D plot (b) contour plot (c) 2D plot

Figure 5: The wave profile representing periodic solution for Eq. (79), (a) 3D plot (b) Contour plot (c) 2D plot, when $p = -3.5,\ q = -3,\ k_1 = 2,\ k_2 = 0.9,\ d_0 = 1.5,\ \Xi = 0.5$

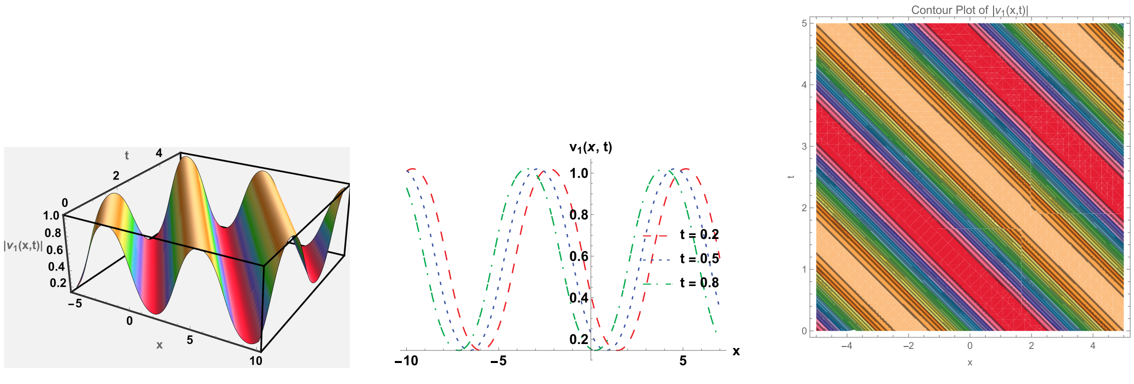

(a) 3D plot (b) contour plot (c) 2D plot

Figure 6: The wave profile representing periodic solution for Eq. (79), (a) 3D plot (b) contour plot (c) 2D plot, when $p = -3.5$, $q = -3$, $k_1 = -2$, $k_2 = 0.9$, $d_0 = 1.5$, $\Xi = 0.5$

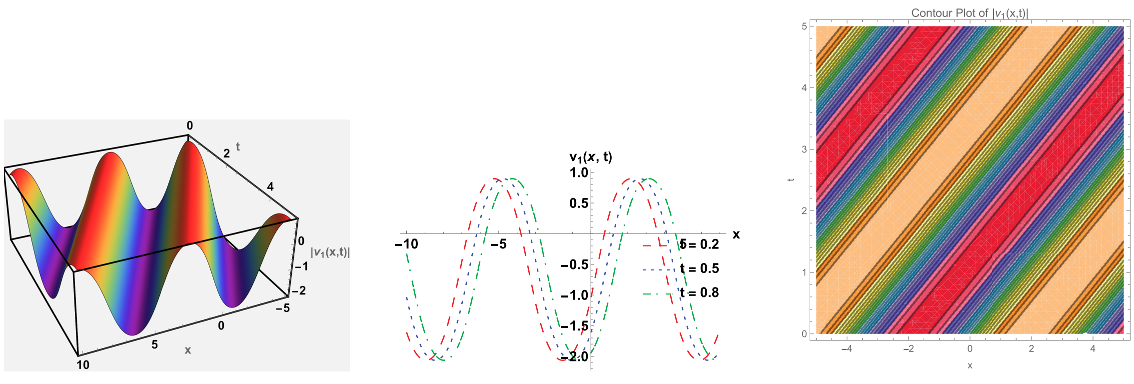

(a) 3D plot (b) contour plot (c) 2D plot

Figure 7: The wave profile representing periodic solution for Eq. (80), (a) 3D plot (b) Contour plot (c) 2D plot, when $p = 0.9$, $q = 0.3$, $k_1 = -2$, $k_2 = 0.9$, $d_0 = 1.5$

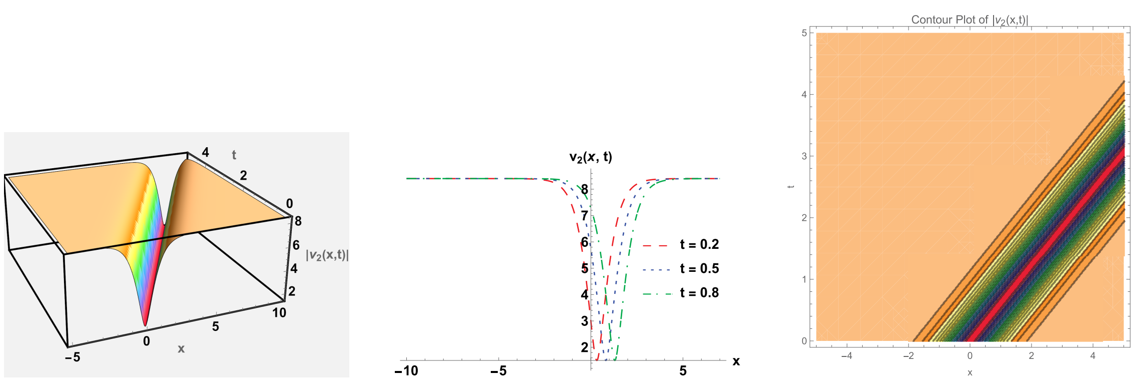

(a) 3D plot (b) contour plot (c) 2D plot

Figure 8: The wave profile of v_2 solution representing dark solution for Eq. (81), (a) 3D plot (b) Contour plot (c) 2D plot, when $p = 0.9$, $q = 0.3$, $k_1 = -2$, $k_2 = 0.9$, $d_0 = 1.5$, $\Xi = 0.5$

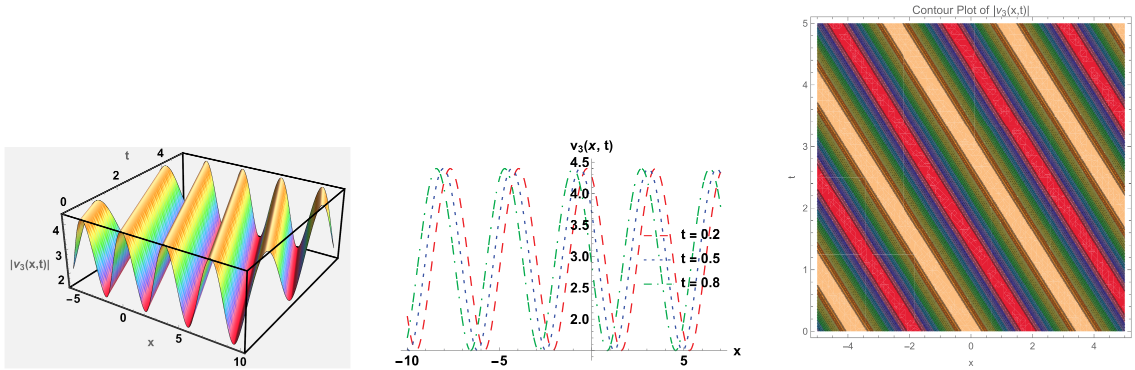

(a) 3D plot (b) contour plot (c) 2D plot

Figure 9: The wave profile of v_3 solution representing periodic soliton for Eq. (82), (a) 3D plot (b) Contour plot (c) 2D plot, when $p = 0.9,\ q = 0.3,\ k_1 = -2,\ k_2 = 0.9,\ d_0 = 1.5,\ \Xi = 0.5$

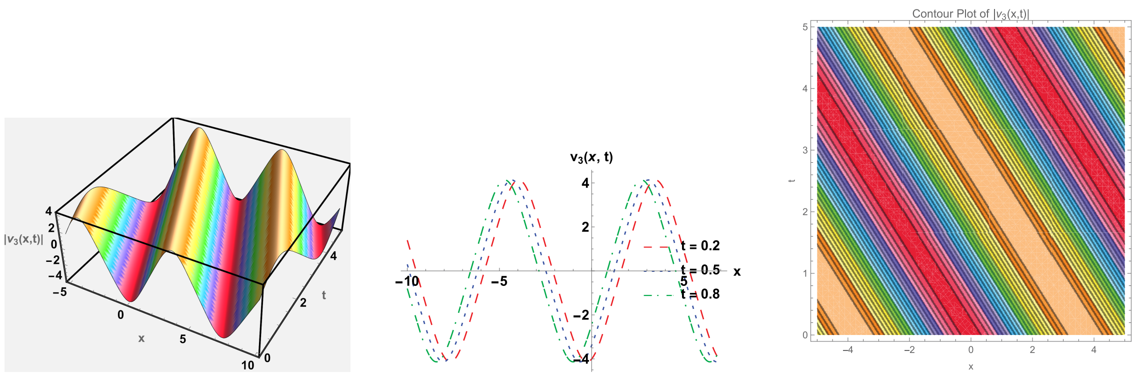

(a) 3D plot (b) contour plot (c) 2D plot

Figure 10: The wave profile of v_3 solution representing periodic soliton for Eq. (82), (a) 3D plot (b) Contour plot (c) 2D plot, when $p = 0.9,\ q = 0.3,\ k_1 = -2,\ k_2 = 0.9,\ d_0 = 1.5$

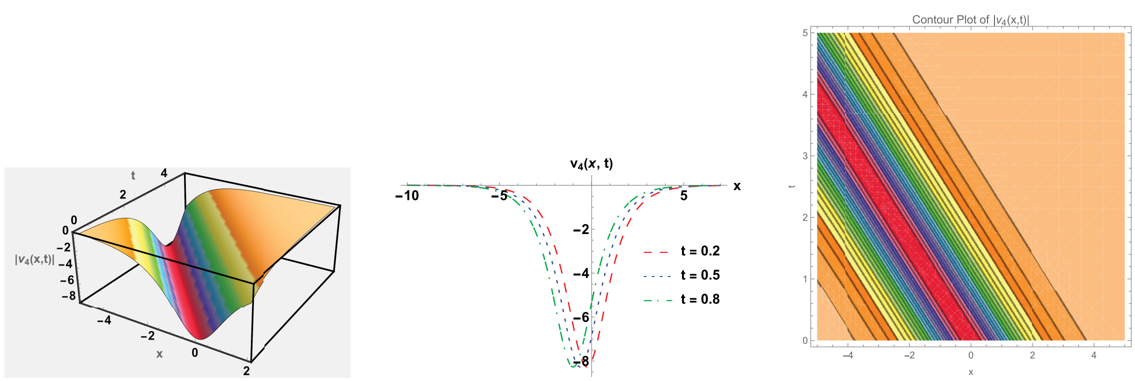

(a) 3D plot (b) contour plot (c) 2D plot

Figure 11: The wave profile of v_4 solution representing dark soliton for Eq. (83), (a) 3D plot (b) Contour plot (c) 2D plot, when $p = 0.9,\ q = 0.3,\ k_1 = -2,\ k_2 = 0.9,\ d_0 = 1.5$

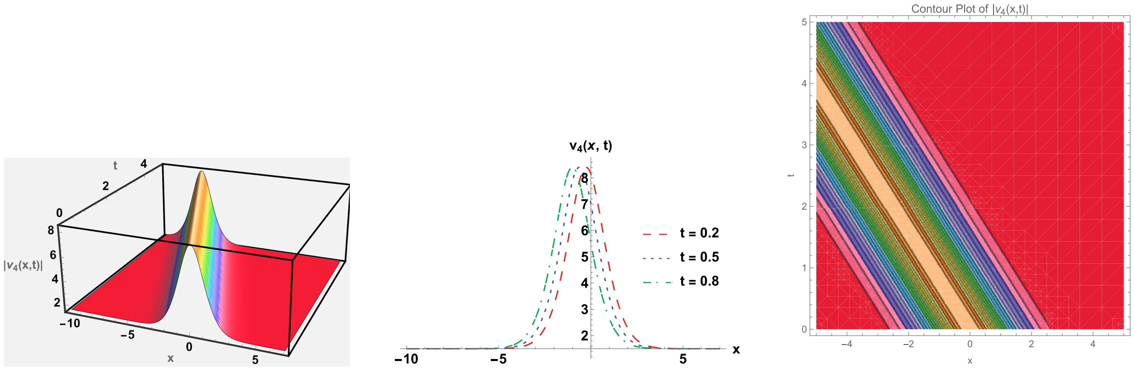

(a) 3D plot (b) contour plot (c) 2D plot

Figure 12: The wave profile of v_4 solution representing bright soliton for Eq. (83), (a) 3D plot (b) Contour plot (c) 2D plot, when $p = 0.9$, $q = 0.3$, $k_1 = 0.2$, $k_2 = 0.9$, $d_0 = 1.5$

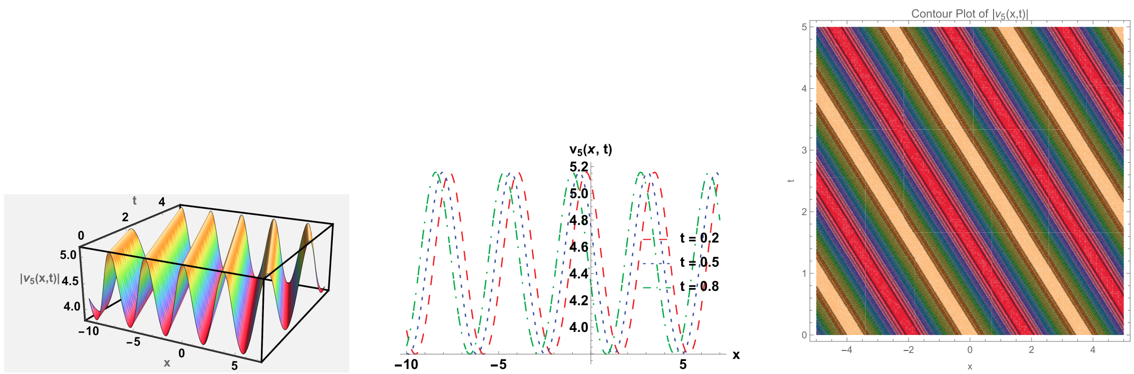

(a) 3D plot (b) contour plot (c) 2D plot

Figure 13: The wave profile of v_5 solution representing periodic soliton for Eq. (84), (a) 3D plot (b) Contour plot (c) 2D plot, when $p = 2.9$, $q = 0.3$, $k_1 = -2$, $k_2 = 6$, $d_0 = 1.5$

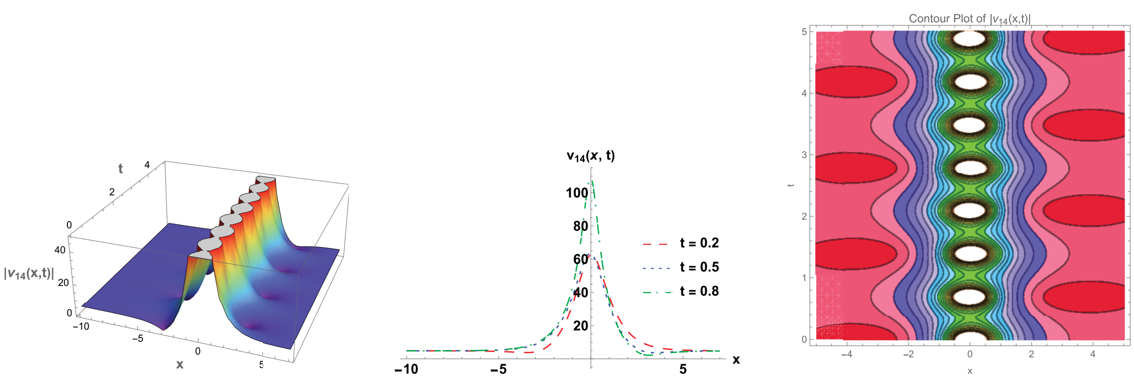

(a) 3D plot (b) contour plot (c) 2D plot

Figure 14: The wave profile of v_{14} solution representing bright soliton for Eq. (93), (a) 3D plot (b) Contour plot (c) 2D plot, when $p = 2.9$, $q = 0.3$, $k_1 = -2$, $k_2 = 0.6$, $d_0 = 1.5$, $\Xi = 0.5$

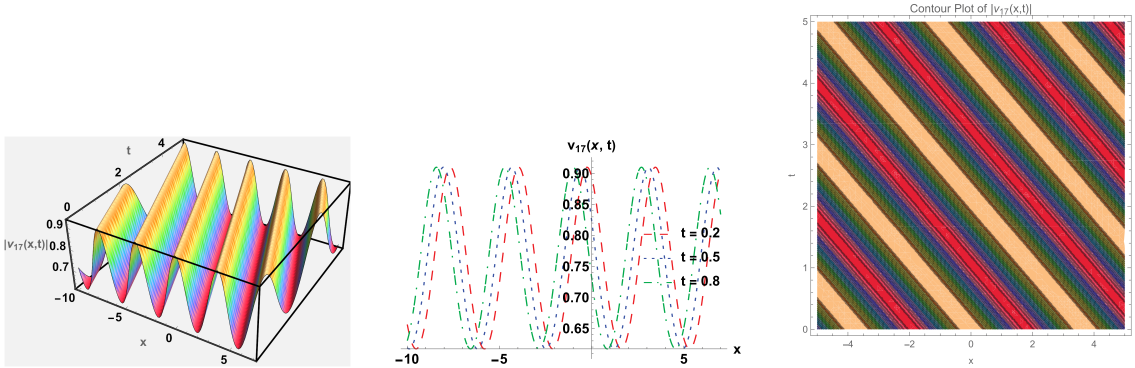

(a) 3D plot (b) contour plot (c) 2D plot

Figure 15: The wave profile of v_{17} solution representing dark soliton for Eq. (96), (a) 3D plot (b) Contour plot (c) 2D plot, when $p = -0.9,\ q = 0.3,\ k_1 = 0.2,\ k_2 = 0.6,\ d_0 = 1.5$

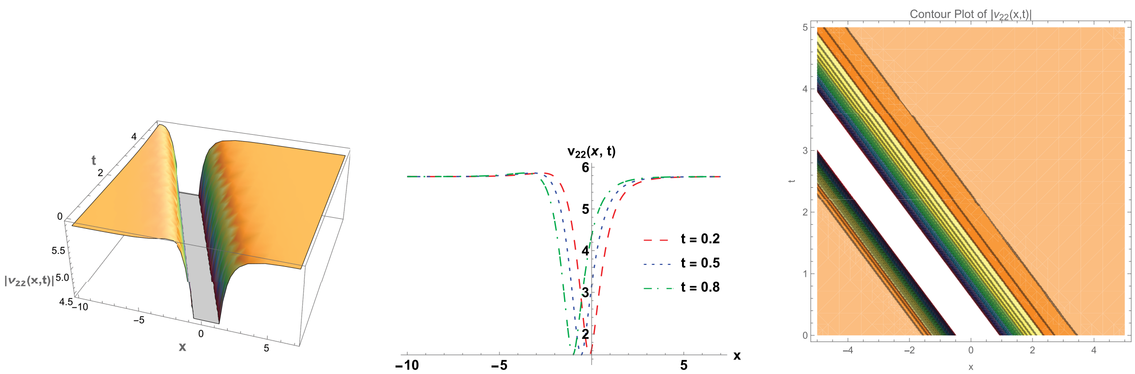

(a) 3D plot (b) contour plot (c) 2D plot

Figure 16: The wave profile of v_{22} solution representing dark soliton for Eq. (101), (a) 3D plot (b) Contour plot (c) 2D plot, when $p = -0.9,\ q = 0.3,\ k_1 = 0.2,\ k_2 = 0.6,\ d_0 = 1.5$

Comparison Analysis

In this section, we will compare our results with existing literature with the help of Table 3.

Table 3: Comparison analysis of our solutions with [47]

Solutions in [47]	Our solutions
(i) Utilized the Exp $(-\phi(\xi))$ function method.	(i) Utilized Khater method and JEFM.
(ii) These solutions include trigonometric and hyperbolic trigonometric solutions.	(ii) These solutions included exponential, rational, hyperbolic and trigonometric forms.
(iii) Soliton solutions with kink and periodic shapes are produced by considering the suggested method.	(iii) The bell, anti-bell, periodic, anti-kink, and kink soliton are produced.

6 Conclusions

In summary, this research successfully evaluated the nonlinear characteristics of the Boussinesq-type equation featuring amplitude-dependent nonlinearity through analytical methods, such as the Khater approach and the JEFM. A variety of accurate soliton solutions have been obtained, illustrating different structural dynamics including kink, anti-kink, periodic, dark, and bright shaped waveforms. The 2D, 3D, and contour plots provided direct visual representations of the behavior of the solutions. The most important point regarding our work is that it provides a novel biological basis for the mechanical wave behaviour of biomembranes, specifically for membrane systems of nerve fibres. Our model differs from classical electrical theories of nerve impulse transmission, and is consistent with the Heimburg–Jackson hypothesis, which allows biological solitons—self-sustained, localized mechanical pulses to propagate along the lipid bilayer as a result of nonlinearity and dispersion. Biological solitons do not have to be just a mathematical abstraction; they have a physical meaning supported by experimental evidence. Generally, biological solitons are attractive as a model for mechanical signalling within living systems since they are stable, robust, and shape-preserving. Our solutions also provide a foundation for dimension-building to investigate pulse interactions, memory effects, and signal modulation in soft biological media. In summary, this work not only add to the mathematical theory of nonlinear wave equations, it allows a direct link between analytic soliton theory and present day biophysics. Furthermore, the techniques employed in this work are very flexible and could be applied to more complex fractional-order systems, as well as, multi-dimensional models or systems with variable coefficients. To the best of our knowledge, the biological solitons of considered mdodel have not been reported by using the proposed techniques in literature.

Acknowledgement: Not applicable.

Funding Statement: The authors received no external funding for this study.

Author Contributions: Fiazuddin Zaman: Software, Investigation, Visualization, Writing—Original Draft, Supervision. Fazal Abbas: Formal Analysis, Visualization, Writing—Original Draft, Writing—Review Editing. Ali Raza: Formal Analysis, Methodology, Investigation, Visualization, Writing—Original Draft, Writing—Review Editing. Sajawal Abbas Baloch: Formal Analysis, Methodology, Software, Investigation, Visualization, Writing—Original Draft, Writing—Review Editing. All authors reviewed the results and approved the final version of the manuscript.

Availability of Data and Materials: All data generated or analyzed during this study are included in this manuscript.

Ethics Approval: Not applicable.

Conflicts of Interest: The authors declare no conflicts of interest to report regarding the present study.

References

1. Liu X, Cai X, Huang Z, Hou Y, Qin J, Chen Z. Comparative study on the oblique water-entry of high-speed projectile based on rigid-body and elastic-plastic body model. Def Technol. 2025;46(2):133–55. doi:10.1016/j.dt.2024.11.007.
2. Bo Y, Tian D, Liu X, Jin Y. Discrete maximum principle and energy stability of the compact difference scheme for two dimensional allen cahn equation. J Funct Spaces. 2022;2022(1):8522231.

3. Jiang P, Zheng H, Xiong J, Rabczuk T. The localized radial basis function collocation method for dendritic solidification, solid phase sintering and wetting phenomenon based on phase field. J Comput Phys. 2025;520(8–9):113515. doi:10.1016/j.jcp.2024.113515.
4. Usman M, Hussain A, Farooq MU, Herrera J. Group analysis of a class of nonlinear wave equations. Eur J Pure Appl Math. 2025;18(4):6128–8.
5. Farooq MU, Hussain A, Farooq MU. Lie group method and its invariants for the extended (3+ 1)-dimensional dispersive Kairat-X equation. Pramana. 2025;99(4):160. doi:10.1007/s12043-025-03005-3.
6. Raza N, Rafiq MH, Kaplan M, Kumar S, Chu YM. The unified method for abundant soliton solutions of local time fractional nonlinear evolution equations. Results Phys. 2021;22:103979.
7. Kumar A, Kumar S. Dynamic nature of analytical soliton solutions of the (1+ 1)-dimensional Mikhailov-Novikov-Wang equation using the unified approach. Int J Math Comput Eng. 2023;1(2):217–28. doi:10.2478/ijmce-2023-0018.
8. Wang S. Novel soliton solutions of CNLSEs with Hirota bilinear method. J Opt. 2023;52(3):1602–7. doi:10.1007/s12596-022-01065-x.
9. Wazwaz AM. Multiple-soliton solutions for the KP equation by Hirota's bilinear method and by the tanh-coth method. Appl Math Comput. 2007;190(1):633–40. doi:10.1016/j.amc.2007.01.056.
10. Ibrahim S, Ashir AM, Sabawi YA, Baleanu D. Realization of optical solitons from nonlinear Schrödinger equation using modified Sardar sub-equation technique. Opt Quantum Electron. 2023;55(7):617. doi:10.1007/s11082-023-04776-y.
11. Zayed EM, Al-Nowehy AG. Solitons and other solutions to the nonlinear Bogoyavlenskii equations using the generalized Riccati equation mapping method. Opt Quantum Electron. 2017;49(11):359. doi:10.1007/s11082-017-1195-0.
12. Kopçasız B. Unveiling new exact solutions of the complex-coupled Kuralay system using the generalized Riccati equation mapping method. J Math Sci Model. 2024;7(3):146–56.
13. Islam SR. Bifurcation analysis and exact wave solutions of the nano-ionic currents equation: via two analytical techniques. Results Phys. 2024;58(1):107536. doi:10.1016/j.rinp.2024.107536.
14. Hossain R, Sagib M, Hossain MA, Islam SR. Soliton solutions, bifurcation, sensitivity and chaotic analysis of the nonlinear combined Kairat-II-X wave model. Phys Lett A. 2025;562(10):131010. doi:10.1016/j.physleta.2025.131010.
15. Wang Y, Zhai W, Li J, Liu H, Li C, Li J. Friction behavior of biodegradable electrospun polyester nanofibrous membranes. Tribol Int. 2023;188:108891.
16. Yu W, Wang P, Zhao M, Qu Y, Du X. Fluid-structure interaction simulation of floating structure interacting with the combined effect of wave-current-earthquake based on CFD method. Ocean Eng. 2025;339(6):122192. doi:10.1016/j.oceaneng.2025.122192.
17. Liu X, Zhao L, Jin J. A noise-tolerant fuzzy type zeroing neural network for robust synchronization of chaotic systems. Concurr Comput. 2024;36(22):e8218.
18. Tang Y, Li Y, Chen P, Zhong S, Yang Y. Nucleic acid aptamer based sensors for bacteria detection. BioEssays. 2025;47(3):e202400111.
19. Su M, Tang T, Tang W, Long Y, Wang L, Liu M. Astragalus improves intestinal barrier function and immunity by acting on intestinal microbiota to treat T2DM: a research review. Front Immunol. 2023;14:1243834. doi:10.3389/fimmu.2023.1243834.
20. Hassan FU, Liu C, Mehboob M, Bilal RM, Arain MA, Siddique F, et al. Potential of dietary hemp and cannabinoids to modulate immune response to enhance health and performance in animals: opportunities and challenges. Front Immunol. 2023;14:1285052. doi:10.3389/fimmu.2023.1285052.
21. Zhang GY, Ma LL, Lin E, Wang ZY, Pan JT, Yang J, et al. Periodically-modulated unipolar and bipolar orders in nematic fluids towards miniaturized nonlinear vectorial optics. Nat Commun. 2025;16(1):9419. doi:10.1038/s41467-025-64463-2.

22. Qiao C, Long X, Yang L, Zhu Y, Cai W. Calculation of a dynamical substitute for the real Earth-Moon system based on Hamiltonian analysis. Astrophys J. 2025;991(1):46.
23. Guo X, Zhang J, Meng X, Li Z, Wen X, Girard P, et al. HALTRAV: design of A High-performance and Area-efficient Latch with Triple-node-upset Recovery and Algorithm-based Verifications. IEEE Trans Comput Aided Des Integr Circuits Syst. 2025;44(6):2367–77. doi:10.1109/tcad.2024.3511335.
24. Boussinesq J. Théorie de l’intumescence liquide appelée onde solitaire ou de translation se propageant dans un canal rectangulaire. CR Acad Sci Paris. 1871;72(755–759):1871. (In French).
25. Christov CI, Maugin GA, Porubov AV. On Boussinesq’s paradigm in nonlinear wave propagation. Rep Mechan. 2007;335(9–10):521–35.
26. Maugin GA. On some generalizations of Boussinesq and KdV systems. Proc Estonian Acad Sci Phys Math. 1995;44(1):40–55. doi:10.3176/phys.math.1995.1.04.
27. Maugin GA. Nonlinear waves in elastic crystals. Oxford, UK: Oxford University Press; 1999.
28. Porubov AV. Amplification of nonlinear strain waves in solids. Vol. 9. Singapore: World Scientific; 2003.
29. Berezovski A, Engelbrecht J, Salupere A, Tamm K, Peets T, Berezovski M. Dispersive waves in microstructured solids. Int J Solids Struct. 2013;50(11–12):1981–90.
30. Engelbrecht J, Tamm K, Peets T. On mathematical modelling of solitary pulses in cylindrical biomembranes. Biomech Model Mechanobiol. 2015;14(1):159–67.
31. Engelbrecht J. Nonlinear wave dynamics: complexity and simplicity. Vol. 17. Berlin, Germany: Springer Science & Business Media; 2013.
32. Mindlin RD. Micro-structure in linear elasticity. Arch Ration Mech Anal. 1964;16(1):51–78. doi:10.1007/bf00248490.
33. Heimburg T, Jackson AD. On soliton propagation in biomembranes and nerves. Proc Natl Acad Sci. U S A 2005;102(28):9790–5.
34. Debanne D, Campanac E, Bialowas A, Carlier E, Alcaraz G. Axon physiology. Physiol Rev. 2011;91(2):555–602.
35. Mueller JK, Tyler WJ. A quantitative overview of biophysical forces impinging on neural function. Phys Biol. 2014;11(5):051001.
36. Hodgkin AL, Huxley AF. A quantitative description of membrane current and its application to conduction and excitation in nerve. J Physiol. 1952;117(4):500.
37. Iwasa K, Tasaki I, Gibbons RC. Swelling of nerve fibers associated with action potentials. Science. 1980;210(4467):338–9.
38. Tasaki I. A macromolecular approach to excitation phenomena: mechanical and thermal changes in nerve during excitation. Physiol Chem Phys Med NMR. 1988;20(4):251–68.
39. Heimburg T, Jackson AD. On the action potential as a propagating density pulse and the role of anesthetics. Biophys Rev Lett. 2007;2(1):57–78.
40. Andersen SS, Jackson AD, Heimburg T. Towards a thermodynamic theory of nerve pulse propagation. Prog Neurobiol. 2009;88(2):104–13.
41. Appali R, Van Rienen U, Heimburg T. A comparison of the Hodgkin-Huxley model and the soliton theory for the action potential in nerves. In: Advances in planar lipid bilayers and liposomes. Vol. 16. Amsterdam, The Netherlands: Academic Press; 2012. p. 275–99.
42. Maurin F, Spadoni A. Wave propagation in periodic buckled beams. Part I: analytical models and numerical simulations. Wave Motion. 2016;66(2):190–209. doi:10.1016/j.wavemoti.2016.05.008.
43. Maurin F, Spadoni A. Wave propagation in periodic buckled beams. Part II: experiments. Wave Motion. 2016;66:210–9.
44. Bibi S, Mohyud-Din ST, Khan U, Ahmed N. Khater method for nonlinear Sharma Tasso-Olever (STO) equation of fractional order. Results Phys. 2017;7(9):4440–50. doi:10.1016/j.rinp.2017.11.008.

45. Khater MM, Seadawy AR, Lu D. Elliptic and solitary wave solutions for Bogoyavlenskii equations system, couple Boiti-Leon-Pempinelli equations system and Time-fractional Cahn-Allen equation. Results Phys. 2017;7(3):2325–33. doi:10.1016/j.rinp.2017.06.049.
46. Khan MI, Asghar S, Sabi'u J. Jacobi elliptic function expansion method for the improved modified kortwedge-de vries equation. Opt Quantum Electron. 2022;54(11):734. doi:10.1007/s11082-022-04109-5.
47. Rani A, Shakeel M, Kbiri Alaoui M, Zidan AM, Shah NA, Junsawang P. Application of the Exp $(-\phi(\xi))$-Expansion method to find the soliton solutions in biomembranes and nerves. Mathematics. 2022;10(18):3372.